2008-07-11

An ultrahigh stability, low-noise laser current driver with digital control

Christopher J. Erickson
erickson.cj@gmail.com

Marshall Van Zijll

Greg Doermann

Dallin S. Durfee

Original Publication Citation

Erickson, Christopher J., Marshall Van Zijll, Greg Doermann, and Dallin S. Durfee."An ultrahigh stability, low-noise laser current driver with digital control." Review of Scientific Instruments 79 (28).

An ultrahigh stability, low-noise laser current driver with digital control

Christopher J. Erickson, Marshall Van Zijll, Greg Doermann, and Dallin S. Durfee
Department of Physics and Astronomy, Brigham Young University, Provo, Utan 84602, USA

(Received 30 April 2008; accepted 8 June 2008; published online 11 July 2008)

We present a low-noise, high modulation-bandwidth design for a laser current driver with excellent long-term stability. The driver improves upon the commonly used Hall–Libbrecht design. The current driver can be operated remotely by way of a microprocessing unit, which controls the current set point digitally. This allows precise repeatability and improved accuracy and stability. It also allows the driver to be placed near the laser for reduced noise and for lower phase lag when using the modulation input. We present the theory of operation for our driver in detail, and give a thorough characterization of its stability, noise, set-point accuracy and repeatability, temperature dependence, transient response, and modulation bandwidth. © *2008 American Institute of Physics.*
[DOI: 10.1063/1.2953597]

I. INTRODUCTION

Diode lasers have come to play a fundamental role in experimental physics. Their low cost, efficiency, and small size, among other things, have made them a standard part of many experiments.[1] While many turn-key extended-cavity diode laser (ECDL) systems are presently available, they are typically much more expensive than the cost of the parts required to build a custom system, and they are not easily serviced when problems arise. Also, it is difficult to modify them for special purposes, and they do not provide the extreme stability and narrow linewidths needed for many applications. As such, many researchers continue to design and build custom ECDLs. In this paper we discuss the design and performance of a precision current driver, one of the key components in any ECDL system.

The laser current controller we present was designed to meet the specifications needed for the master laser of an optical frequency standard, one of the most demanding ECDL applications. Optical frequency standards require a laser with a linewidth of a few kilohertz or less. To achieve this, these lasers need to have the current stabilized to within a few tens of nanoamperes rms over relevant time scales, and typically must be locked to a high-finesse cavity. To simplify the lock to the cavity, it is desirable for the laser current driver to have a modulation input with enough bandwidth to allow feedback through the current driver. This reduces complexity and reduces the chance of destroying the diode when compared to applying feedback directly to the diode.

Our current driver has several unique design features. The noise and stability of our current driver are as good or better than any laser current driver we are aware of. The current driver also has a modulation input with a 3 dB roll off above 20 MHz. This is much larger than any of the commercial drivers we have seen, and it maintains its high stability and low noise even while the high-bandwidth modulation circuit is active and connected to the driver's output. The driver is also relatively small in size and features remote programming, allowing the driver to be placed near the laser to remove the negative effects of long cables. This design is inexpensive enough to be used as a reliable laboratory standard or in student laboratory experiments.

Our design builds upon the Hall–Libbrecht current driver,[2] a precision current controller design which has been used extensively in atomic physics laboratories. We made several design improvements and updated components. The most radical improvement is the use of a precision digital-to-analog converter (DAC), rather than a potentiometer, to program the current set point. This eliminates a major source of noise and instability. This also makes it possible to program the current set point remotely, allowing the current driver to be placed in close proximity to the laser diode. This can significantly reduce current noise at the laser, and will lower phase shifts when using the modulation input. The use of a DAC also allows much more accurate control of the current set point, and makes it possible to return to a previous current set point with extremely high precision. Our driver utilizes surface-mount technology, allowing us to use the most modern components and reducing inductance and noise pickup from longer pin leads.

In addition to explaining our improvements to the Hall–Libbrecht circuit we present a much more detailed description and a more comprehensive and careful performance analysis of our design than was given in Ref. 2. This discussion illuminates both our improvements as well as subtleties present in the Hall–Libbrecht driver which were not discussed in Ref. 2.

II. DESIGN AND CONSTRUCTION

In Fig. 1 we have broken the schematic of the circuit into several sections, which we will address separately. As presented, the circuit is configured to drive cathode grounded lasers, but we have also constructed anode-grounded supplies with a few straightforward modifications. Although not indicated on the schematic, each op-amp is powered by the filtered voltages V_p and V_n, with a pair of capacitors connected between power and ground near each power pin of each op-amp. Surface-mount ceramic capacitors 0.01 and 10 μF in value are used for the op-amps in the "modulation

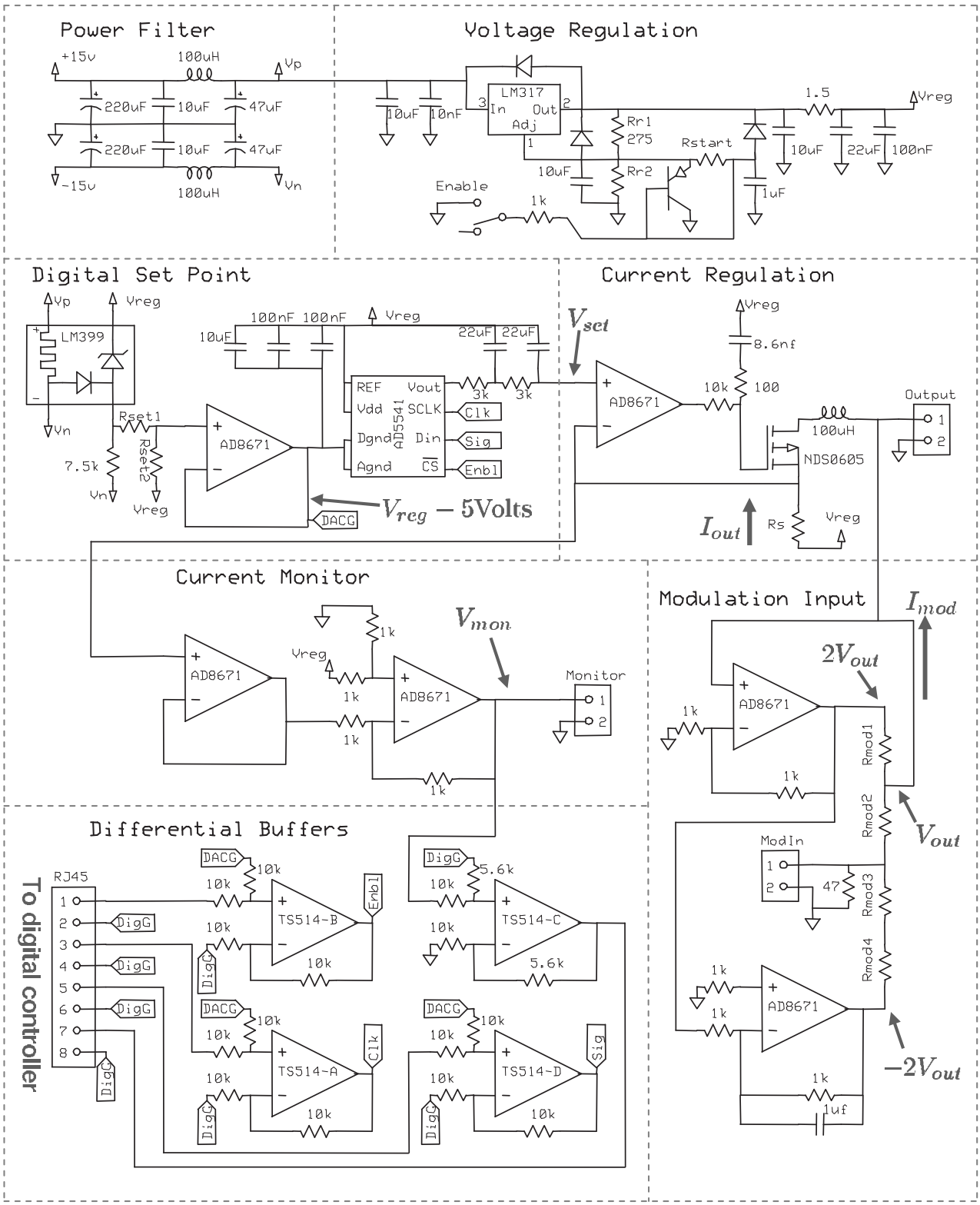

FIG. 1. Schematic of the laser diode current driver circuit. The circuit is divided in to separate functions for clarification and easy refrencing.

input" subcircuit, the quad op-amp in the "differential buffers" subcircuit, and the op-amp used for the differential amplifier in the "current monitor" subcircuit. For the power lines of the other three op-amps a 0.1 μF ceramic capacitor and a 100 μF electrolytic capacitor are used. The circuit is laid out on a 6.125×4.25 in.^{2} printed circuit board (PCB) that is electrically isolated from the cast aluminum box it is mounted in. All of the resistors, with the exception of the ones specifically discussed in the sections below, are standard 1/8 W thick-film chip resistors with a temperature coefficient of ± 200 ppm/ °C in a 1206 surface-mount package. All of the nonpolar capacitors are ceramic capacitors in a 1206 surface-mount package. Other components are discussed later.

A. Current regulation

The heart of the current driver is the "current regulation" subcircuit. This subcircuit is a fairly standard current source design,[3] but components have been chosen very carefully for optimal performance. In this sub-circuit a regulated voltage, labeled V_{reg} in Fig. 1, is used to drive current through a precision sense resistor, labeled R_s, to the output of the driver. The amount of current flowing out to the laser diode can be determined from the voltage drop across R_s. One side of the sense resistor is connected to the inverting input of an AD8671 precision op-amp, and the output of the op-amp is connected to the gate of an NDS0605 metal-oxide-semiconductor field-effect transistor (MOSFET). Negative feedback in this circuit causes the MOSFET gate voltage to change, modifying the current flowing through the MOSFET, until the voltage at the output of the sense resistor is equal to the set voltage, V_{set}, applied to the noninverting input of the op-amp. In this way the op-amp forces the current to remain fixed at a value of

$$I = \frac{V_{reg} - V_{set}}{R_s} \quad (1)$$

regardless of the load impedance. Due to the MOSFET's gate capacitance, the resistors and capacitor on the line between the op-amp and the MOSFET are needed to reduce the bandwidth of the circuit and prevent oscillations. As was done in Ref. 2, an inductor is placed after the MOSFET to limit high frequency current noise and to decouple the current regulation electronics from any intentionally applied current modulation.

The sense resistor is a key component which needs to be considered carefully—stability of the current driver can be no better than the stability of this resistor. The value for R_s should be chosen to provide a large enough voltage drop for accurate current regulation at the target current, but small enough such that the voltage drop across this resistor does not reduce the compliance voltage of the driver below what is necessary to power the laser diode. When driving a red diode laser to a maximum current of 100 mA, we used a pair of 100 Ω Vishay SMR3D precision resistors in parallel for a total resistance of 50 Ω. These parts are surface-mount components for reduced noise pickup and have a low temperature coefficient of just 2 ppm/ °C. For higher/lower current applications, smaller/larger resistance values could be used. In applications that do not require the highest stability, resistors with higher temperature coefficients may be used.

The op-amp we used was the AD8671 from Analog Devices.[4] Similar to the LT1028 used in the original Hall design,[5] this op-amp has voltage noise levels comparable to the Johnson noise of a 50 Ω resistor, the AD8671 having slightly better current noise and slightly poorer voltage noise than the LT1028. In practice, as well as in numerical SPICE models, we found that the AD8671 was less prone to oscillate in this circuit than the LT1028, requiring less severe bandwidth limiting to make the circuit stable. The AD8671 chip also has a *much* higher input impedance (both common and differential mode) than the LT1028 with comparable input capacitance. This property limits current drift due to thermal or other changes in the leakage current into the op-amp inputs. In addition, the AD8671 does not require any sort of trim or compensation to achieve low bias and low overshoot in our application.

Although the AD8671 has a somewhat smaller gain-bandwidth product than the LT1028 used in the original Hall design (10 versus 50 MHz), the filtering capacitors and resistors needed to stabilize the circuit effectively remove any additional bandwidth that would be gained by using the LT1028. Furthermore, the inherent low noise of the circuit and the use of the decoupling inductor makes higher bandwidth in this part of the circuit unnecessary.

It is worth noting here that we have used the AD8671 op-amps throughout most of the circuit. The Hall design used LT1028 op-amps only in two "critical" locations, with different op-amps being used in the modulation input circuit and the monitoring circuit. Since both of these circuits connect directly to the current output, it made sense to us to take advantage of the low noise and high input impedance of the AD8671. Though more expensive than many lower performance op-amps, they are still a relatively inexpensive part of this circuit.

For the inductor we choose a 100 μH API Delevan series S1210 ferrite core shielded surface-mount inductor. The NDS0605 MOSFET was chosen for its low on-state resistance and a relatively large current carrying capacity in a small form factor. It also has a small input capacitance, small switching delays, and low gate-body leakage.

B. Digital set point

The set-point voltage, V_{set}, which is applied to the noninverting input of the op-amp in the current regulation subcircuit is generated by a precision DAC. Using a precision DAC rather than a manual potentiometer removes a significant source of noise and drift in the circuit. In addition, it affords much greater accuracy and repeatability. We did an extensive search to find a DAC which would optimize long-term stability. The chip we settled on is the 16 bit AD5541.[6] This chip comes in several performance grades. All grades have the same stability, temperature coefficient, and repeatability, but differ in the absolute accuracy of the output. We chose the "J" grade, mainly because it was carried by our regular electronics supplier, but lower cost/lower performance and higher cost/higher performance grades are also available. For applications where the noise and stability of the current driver are not a great concern, we have included pads on the PCB where a traditional potentiometer can be used in place of the DAC.

The AD5541 chip is specified to have a zero-code temperature coefficient of 0.05 ppm/ °C and a gain error temperature coefficient of 0.1 ppm/ °C, both of which are significantly less than the temperature coefficient of the sense resistors discussed in Sec. II A. The accuracy of the J grade chip is guaranteed to be at least as good as ±2 times the least significant bit (LSB), or two parts in 65 535. For our test setup we used a 50 Ω sense resistor resulting in a maximum current output of 100 mV. This corresponds to an accuracy of ±3 μA, similar to its measured accuracy discussed in Sec. III B.

The output of the DAC can be set anywhere from the voltage of its analog ground pin (labeled DACG in Fig. 1) up to the voltage applied to its reference input. As was done with the analog potentiometer used in Ref. 2, the ground pin of the DAC in our circuit is not connected directly to board ground. There are two reasons why this is necessary. The first is that the output current of the circuit does not depend on the set-point voltage relative to board ground, but relative to V_{reg}. As such, if the voltage V_{reg} drifts relative to board ground, we want V_{set} to drift with it such that $V_{\mathrm{reg}}-V_{\mathrm{set}}$ remains constant. The second is that the DAC requires the voltage on its reference to be no greater than 5 V above the voltage of its analog ground pin. In order to adjust the output current of the device all they way down to zero, it must be possible to make V_{set} at least as large as V_{reg}. This imposes a lower limit on the voltage applied to the analog ground pin.

In our circuit V_{reg} is applied directly to the DAC's reference pin, and a voltage of $V_{\mathrm{reg}}-5$ V (labeled DACG in Fig. 1) is applied to the DAC's ground pin, giving the current driver an output current which can range from 0 to 5 V$/R_s$. The voltage DACG, is generated using an LM399 Zener diode connected to V_{reg}, which creates an extremely stable 6.95 V drop. The resistors $R_{\mathrm{set1}}=1$ kΩ and $R_{\mathrm{set2}}=2.74$ kΩ make a voltage divider to lower this 6.95 V difference closer to the required 5 V. We then buffer the voltage with an op-amp. Any drift in the ratio of R_{set1} and R_{set2} will result in a drift in the current set point, but there is much less sensitivity to thermal drift in these resistors than in the sense resistor R_s because only the ratio, and not the absolute resistance matters. Both resistors are made of the same material and are in close proximity such that they will have similar thermal drifts. For these two resistors we use Vishay TNPW0805 precision resistors which have an accuracy tolerance of 0.1% and a thermal coefficient of 25 ppm/°C. The 7.5 kΩ resistor in this subcircuit is a Vishay TNPW04027501DT9 precision, low temperature coefficient resistor. We expect, however, that using a standard resistor in this location would not affect the performance of the current driver.

Similar to what was done in Ref. 2, a pair of low-pass filters reduce high frequency noise in V_{set}. Because the output current of the circuit depends not on the difference of V_{set} from board ground, but on the difference between V_{set} and V_{reg}, these filters (as well as the low-pass filter in the current regulation subcircuit) are tied to V_{reg} rather than ground.

C. Voltage filtering and regulation

The "power filter" subcircuit generates stable, filtered voltages for the rest of the circuit. This subcircuit is nearly identical to the one in Ref. 2. We have added some additional filter capacitors, changed some component values to optimize performance, and added two protection diodes between the three pins of the LM317 voltage regulator, as recommended by the manufacturer.[7] We have also used surface-mount components wherever possible to reduce noise and stray inductance.

In this part of the circuit, power lines are first filtered by a series of capacitors and inductors to provide the positive and negative voltages V_p and V_n which are used to power all of the op-amps in the circuit. The filtered power is then regulated with the LM317 adjustable voltage regulator to generate the extremely stable voltage labeled V_{reg}. This voltage is used to drive current to the laser diode in the current regulation subcircuit and to generate the set-point voltage in the "digital set point" subcircuit as described above.

The transistor below the LM317 is part of an enable/slow start mechanism discussed in Ref. 7. This soft-start feature helps protect the laser diode from damage, and in the case of a power failure it also allows the digital controller time to reset the current set point before V_{reg} turns fully on after power is restored. The regulated output level of the LM317 is nominally equal to

$$V_{\mathrm{reg}} = 1.25\ \mathrm{V}(1 + R_{r2}/R_{r1}). \tag{2}$$

When the *enable* switch is grounded, the current driver is "disabled." In this case the resistor R_{r2} is placed in parallel with both the impedance of the transistor and with the series resistance of the resistor labeled R_{start} and the 1 kΩ resistor near the switch. This effectively reduces the value of R_{r2} in Eq. (2). With a proper choice of resistor values it is possible to make V_{reg} insufficiently large to forward bias the laser diode when the switch is in this position.

When the switch is opened, if not for the 1 μF capacitor, current would immediately cease to flow through R_{start}. This would cause the voltage at the gate of the transistor to suddenly equal the voltage at the emitter of the transistor, shutting off current through the transistor as well, restoring the voltage regulator to its full output value as if the soft-start circuitry was not present. The presence of the 1 μF capacitor prevents the current flowing through R_{start} from abruptly stopping. Instead, the current continues to flow as the capacitor charges, and the voltage rises on the gate of the transistor slowly. This causes the voltage regulator's output to gradually increase to its final value. Because of the nonlinear nature of the transistor, the start time is considerably larger than just the *RC* time constant of the resistor R_{start} and the 1 μF capacitor. Using a value of $R_{\mathrm{start}}=1$ kΩ and a MMBT2907A transistor in our setup, we measured a start-up time constant of 11.5 ms.

The 220 μF capacitors are low-leakage radial aluminum electrolytic capacitors, and the 47 μF capacitors are surface-mount tantalum capacitors. While developing this circuit the 1.5 Ω resistor in the upper right-hand corner of the schematic overheated, probably due to increased current draw when our LT1028 op-amps oscillated or saturated. While diagnosing this problem, we installed a Vishay WSC-1 Series 1 W surface-mount wire-wound power resistor. We have experienced no such difficulties since we began using AD8671 op-amps, and have since replaced this resistor with a standard 1/8 W metal film resistor. Although we do not expect the choice of resistor to affect performance, one should note that the wire-wound resistor was still installed while taking the data presented in Sec. III.

D. Modulation input

The modulation input subcircuit is the same one used and described in Ref. 2. The key components in this circuit are the upper op-amp and the two resistors labeled R_{mod1} and R_{mod2} (the lower op-amp is part of a balancing circuit that we

describe later). The noninverting input of the upper op-amp is connected directly to the output of the current driver, which is at a voltage V_{out}. The op-amp is wired to generate a gain of +2, such that it generates a voltage of $2V_{out}$ at its output. The output of the op-amp is connected to the current driver's output through a 1 kΩ resistor, labeled R_{mod1} in Fig. 1. The voltage drop across this resistor is equal to $2V_{out}-V_{out}=V_{out}$, and so the current flowing through this resistor is $V_{out}/1$ kΩ. A second identical resistor, labeled R_{mod2} in Fig. 1 connects the output of the laser driver to the modulation input. If a voltage V_{mod} is applied to this input, the current flowing through this resistor is $(V_{out}-V_{mod})/1$ kΩ. The current which is added to the output of the laser driver is just the difference in these two currents, $V_{mod}/1$ kΩ. This injected current inevitably results in a change in the output voltage of the current driver, but the op-amp constantly corrects its output to keep it equal to $2V_{out}$ as V_{out} changes.

In addition to the modulation current, an additional bias current will be injected by this subcircuit if the R_{mod} resistors are not equally matched or if the gains in the two amplifiers are not correct. For example, if R_{mod1} and R_{mod2} differ by some small fraction $\varepsilon \equiv (R_{mod2}-R_{mod1})/R_{mod1}$, the modulation current injected into the laser will be

$$I_{mod} = \frac{V_{mod}}{R_{mod2}} + \frac{\epsilon V_{out}}{R_{mod_1}(1+\epsilon)}. \tag{3}$$

The bias term (the second term in the above equation) will cause current measurements based on the voltage drop across R_s to be inaccurate. Moreover, if resistances change in time, due to thermal effects, for example, this bias current will change, affecting the stability of the current driver. As such, these resistors need to be well matched and have a fairly low temperature coefficient.

All of the resistors in the modulation input subcircuit except for the 47 Ω impedance matching resistor on the *ModIn* input are Vishay TNPW0805 surface-mount thin-film chip resistors with a resistance tolerance of ±0.1% and a temperature coefficient of 25 ppm/°C. With this accuracy, the bias term in Eq. (3) should be no larger than ~2 μA when driving a typical red laser diode (for which V_{out} ~2 V). Because the resistors R_{mod1} and R_{mod2} have the same composition and are physically close to each other, such that they should be at similar temperatures, we would not expect temperature to have a large effect on the matching of the two resistors. Accordingly, the fact that these resistors have a much larger temperature coefficient than the current sense resistor discussed in Sec. II A should have no significant effect on the stability of the current driver.

The lower op-amp in this subcircuit forces V_{mod} to 0 V when nothing is connected to the modulation input (alternatively, this part of the circuit could be left off, and the modulation input could be shorted to ground or the modulation input subcircuit completely disconnected from the current output when not in use). This op-amp generates a voltage of $-2V_{out}$ which is connected to the modulation input through two more 1 kΩ resistors, labeled R_{mod3} and R_{mod4}. It is easy to see that, if these are perfectly matched to the other two resistors, the voltage at the modulation input will float to zero when nothing is connected to it. If they are not exactly balanced, an additional bias current will be injected into the output of the current driver when the modulation input is floating. Given the precision of these resistors, we would expect this bias to be on the order of 1 μA and we would not expect that temperature drift should be an issue.

Although not discussed in Ref. 2, we have come to realize that this design allows modulation speeds greater than the bandwidth of the op-amps. At very high modulation frequencies one would expect that the op-amp would not be able to follow the changes in V_{out} induced by the oscillating modulation current. In this limit, if we assume that the current driver is connected to a load with impedance Z, that the output of the upper op-amp in this subcircuit settles to twice the time-averaged output voltage, and that $R_{mod1}=R_{mod2}$, Eq. (3) becomes

$$I_{mod} = \frac{V_{mod}}{R_{mod1}}\left(1+\frac{2Z}{R_{mod1}}\right)^{-1}. \tag{4}$$

If $R_{mod1} \gg Z$, then this equation is nearly the same as the low-frequency limit in Eq. (3). If the op-amp is modeled as an ideal op-amp with a low-pass filter with a time constant of τ on its input, it can easily be shown that I_{mod} changes monotonically from its low-frequency value of V_{mod}/R_{mod1} to this high frequency limit as the modulation frequency increases. Using this model, the phase shift of I_{mod} goes to zero in both the low- and high frequency limits, with the largest phase shift, occurring at a frequency of $f=2\pi[R/\tau^2(R+2Z)]$, being equal to

$$\varphi_{max} = \arctan\left(\sqrt{\frac{Z^2}{R(R+2Z)}}\right). \tag{5}$$

Once again, if $R_{mod1} \gg Z$, the maximum phase shift in this simplified model will be very small.

E. Current monitor and differential buffers

The current monitor subcircuit generates a voltage proportional to the output current of the driver so that the output can be monitored. The first op-amp in this subcircuit buffers the voltage at the low-voltage side of the sense resistor R_s with a high input impedance op-amp. This decouples the current monitor output from the current regulation subcircuit so that measurements can be made without significantly affecting the output of the current driver. The second op-amp subtracts this voltage from V_{reg} to produce a voltage relative to the board's ground equal to $V_{mon}=I_{out}R_s$.

Because the output of the current monitor subcircuit is referenced to board ground, attaching a meter to this output could potentially introduce ground noise. Op-amp "C" in the differential buffers subcircuit eliminates this problem, decoupling the meter's ground from the circuit. Similarly, the other three op-amps in this subcircuit decouple the current driver's ground from the grounds of the three digital input lines which program the DAC (labeled Clk, Sig, and Enbl in Fig. 1). These three op-amps are also used to rereference the digital inputs to the ground pin of the DAC (which is not board ground).

F. Microprocessor

The circuit can be controlled by any device capable of generating a 16 bit serial transistor-transistor logic (TTL) signal as well as a TTL clock and enable signal.[6] To collect some of the data presented in this paper, we used a digital output card on a computer for this purpose. We have also developed a dedicated digital control circuit based on a PIC18F4550 microprocessor. This is a 40-pin USB programmable microprocessor with 35 input/output pins. It is programed to read in the signal from a digital encoder, and subsequently output a value to the DAC. The microcontroller maintains stability and eliminates noise pickup by only outputting values to the DAC when the user changes the current set point. The PIC18F4550 also includes a built-in analog to digital converter which we use to read back and display V_{mon}.

G. Output current limitations

To protect the laser diode, it is often desirable to limit the maximum output current of the driver. An easy way to do this is by changing the resistance of the sense resistor, R_s. Because the DAC can only generate a set-point voltage as low as $V_{\mathrm{reg}}-5V$, the maximum output of the current driver will be $5\ \mathrm{V}/R_s$. However, because the modulation current from the modulation input subcircuit does not pass through the sense resistor, it is possible to exceed this maximum current by applying a large enough voltage to the modulation input.

As discussed in Ref. 2, another way to limit the output current is by reducing the voltage V_{reg}. The compliance voltage of the current driver is determined by the impedance of the MOSFET and the inductor in the current regulation subcircuit and the value of V_{reg}. If I_{max} is the maximum current for the laser diode, and if V_{diode}, V_{MOSFET}, and V_L are the voltage drops across the laser diode, the MOSFET, and the inductor (respectively) at this current, then if V_{reg} is set to

$$V_{\mathrm{reg}} = V_{\mathrm{diode}} + V_{\mathrm{MOSFET}} + V_L + I_{\mathrm{max}}R_s, \tag{6}$$

the current driver output will not be able to exceed I_{max}. The above voltage drops can be estimated from the specifications of the components, or the ideal value for V_{reg} can be determined empirically by setting V_{set} to its lowest value and gradually increasing V_{reg} until the output current equals I_{max}. Because an inductor decouples the modulation input subcircuit from the current regulation subcircuit, a high frequency signal on the modulation input could cause the current driver to output more than I_{max}. At low modulation frequencies the output current will never exceed I_{max}, regardless of the amplitude of the voltage applied to the modulation input.

The maximum current that can be generated without risking damage to the current driver is 127 mA (limited by the S1210 inductor). For higher current applications, we designed our circuit boards to accommodate both surface-mount and leaded components at a few critical points, allowing a wide range of components to be used. For example, we have realized a high current driver for a tapered amplifier by replacing the following components: the S1210 inductor (rated for 127 mA) as well as the two inductors in the power filter subcircuit were replaced with leaded 125 μH inductors; the NDS0605 MOSFET (with a maximum rated current of 180 mA) was replaced with an IRF9Z14 MOSFET in a TO-220 package which can output 6.7 A; the surface-mount LM317 regulator (with a current limit of 1 A) was replaced with an LM1084-ADJ regulator in a TO-220 package, which is capable of 5 A; The 1.5 Ω resistor in the "voltage regulation" subcircuit was replaced with a leaded 1 Ω, 5 W power resistor; and the sense resistor R_s was realized with two 5 Ω, 10 W leaded power resistors placed in parallel for a combined resistance of 2.5 Ω. Due to the larger gate capacitance of the MOSFET, we also had to replace the capacitor in the current regulation subcircuit with a 100 nF capacitor to keep the circuit from oscillating. Although these substitutions increase the noise and reduce the stability of the circuit, they allow an output of 2 A (limited intentionally by our choice of R_s to match the capacity of our tapered amplifier).

III. RESULTS

We did a series of tests to characterize the performance of our current driver. For each of these tests, the sense resistor consisted of two 100 Ω resistors in parallel, for a sense resistance of $R_s=50\ \Omega$.

A. Noise and stability

To characterize both the long-term stability and the high frequency noise of the current driver, we used it to drive a laser diode in series with a 2.5 Ω precision resistor with a current of 74.5 mA. The current was determined by measuring the voltage drop across the resistor with a 6.5 digit multimeter. From these data we extracted the spectral density of the current noise, shown in Fig. 2(a). The intrinsic noise of our measuring apparatus was determined by taking a similar measurement but with the current driver disconnected from the laser/2.5 Ω resistor. For most of the spectrum, our driver is at or near the detection limit of our equipment, and at all frequencies it is at least an order of magnitude smaller than the measurements presented in Ref. 2.

The long-term drift in the output current is shown in Fig. 2(b). These data were collected in the same manner as the data used to produce Fig. 2(a), but with a current set point of 74.8 mA. During this measurement thermistors were used to measure the temperature at the location of the current sense resistor (labeled R_s in Fig. 1), the DAC, and the box that houses the current driver. The mean temperatures at these locations were 40.6, 40.5, and 22.9 °C, respectively. As seen in Fig. 2(c), the drifts in current and temperature are highly correlated. These data suggest a temperature coefficient of $\approx$1.7 ppm/°C, precisely what would be expected given the 2 ppm/°C temperature coefficient of the sense resistor.

B. Set-point accuracy and repeatability

The use of a digital set point results in very good accuracy, linearity, and repeatability. We tested the linearity of the set point by connecting our current driver to a laser diode in series with a 10 Ω precision resistor. We then determined the actual current produced by the driver at various digital set points by measuring the voltage drop across the resistor. The deviation of the actual current from a best-fit line is shown in

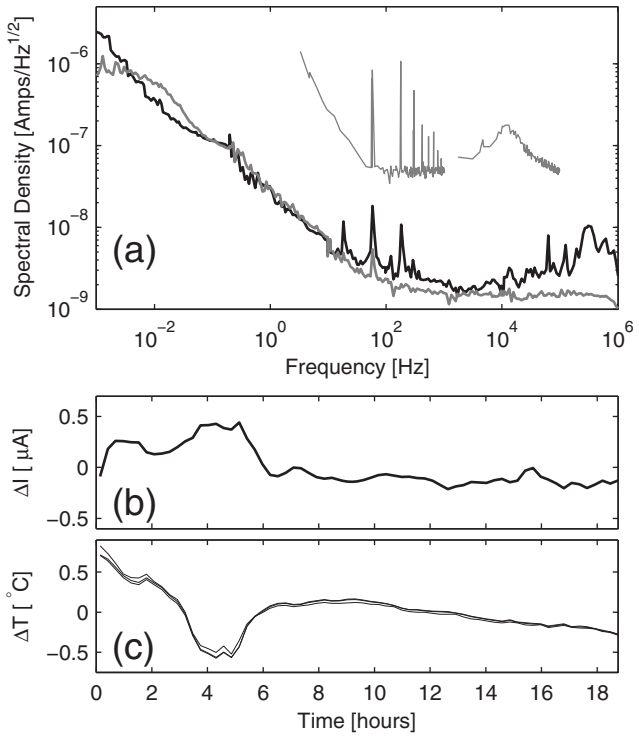

FIG. 2. Noise and drift in the current. In (a) the spectral density of the current noise is shown. The black line represents the spectral density of the current signal when the diode and resistor were driven by the current driver. The thick gray line is the spectral density of the intrinsic noise of the measurement apparatus, measured by disconnecting the current driver from the laser diode. The thin gray lines are the spectral density of the noise data in the original paper on the Hall–Libbrecht design (Ref. 2). In (b) the measured drift of the output current about its mean value is shown as a function of time. In (c) the drift in the temperature at three locations is plotted (all three sets of temperature data are plotted on top of each other).

Fig. 3(a). The linearity is within the ±2 LSB specification for the DAC chip we used. As discussed in Sec. II B, similar chips with higher or lower linearity are available.

The set point repeatability of our circuit is much better than the absolute accuracy. To test the repeatability, the current set point was set digitally, and the actual current was measured. The digital set point was then changed momentarily to significantly increase the output current. The digital set point was then reset to its original value, and the actual current was remeasured. This was done ten times at each digital set point, and the rms deviation of those ten measurements was calculated. The rms deviation is plotted as a function of the digital current set point in Fig. 3(b). As shown in this figure, the set-point repeatability is about 40 nA rms.

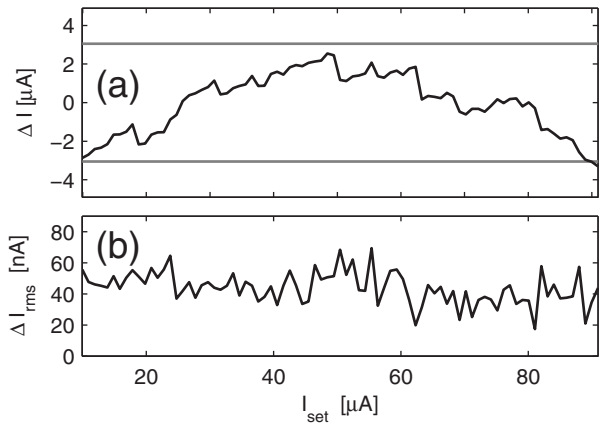

FIG. 3. Accuracy and repeatability of the current set point. The plot in (a) shows the deviation of the actual current data from the set point. The gray lines indicate the ±2 LSB points specified in the DAC's data sheet. Plot (b) show the rms repeatability of the current output, measured as a function of the digitally programed set point.

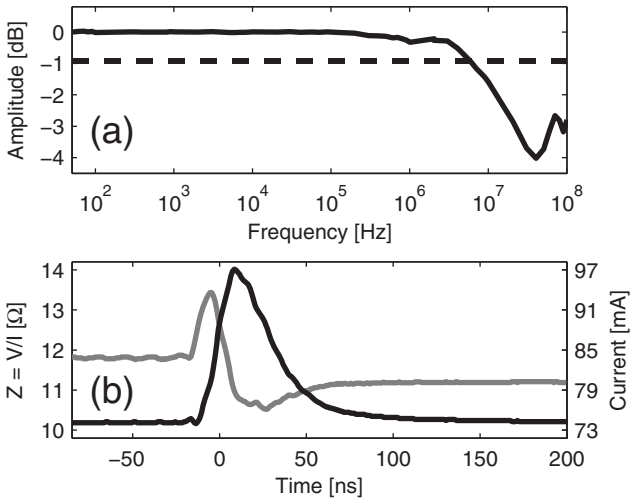

FIG. 4. Temporal response of the current driver. In (a) the Bode plot of the response to the modulation input is displayed. The solid line is the amplitude of the response of the driver normalized to the ideal V_{mod}/R_{mod1} response for the signal applied to the modulation input. The dashed line is the theoretical high frequency response assuming ideal components and transmission lines given by Eq. (4). In (b) the transient response of the current driver to a total load change of roughly 3% is shown. The black line is the current through the load, and the gray line is the impedance of the load.

C. Modulation response

We measured the modulation response of the current driver by terminating the output with a 50 Ω resistor and comparing the amplitude of a sine wave applied to the modulation input of the current driver input to the amplitude of the sinusoidal voltage modulation generated across this resistor. The output amplitude was then normalized to the expected output of $V_{mod}/1\ k\Omega$ to produce the curve shown in Fig. 4(a). We found the 3 dB point to be over 20 MHz, with an attenuation of less than 4 dB out past 100 MHz. We found, however, that the frequency response was severely degraded when driving reactive loads. As discussed in Sec. II D, this is a much better frequency response than one might naively expect based on the bandwidth of the op-amps.

D. Transient response to load impedance variation

The transient response of the current driver was studied by using it to drive current through a 10 Ω resistor in series with a VZN1206 MOSFET. The transistor gate voltage was suddenly changed to vary the overall impedance of the load seen by the current driver. The current was determined from the voltage across the resistor, and the time-varying impedance was calculated by dividing the voltage drop across the entire transistor-resistor circuit by the current found in the resistor. The measurements are shown in Fig. 4(b). The distance between the peaks in the two traces is 14 ns, indicating

a very fast initial response to the impedance change. After 100 ns, the impedance had settled down to a constant value. By fitting the current signal beyond this time to an exponential, we extracted a time constant for the driver's response to small load changes of 70 ns.

IV. CONCLUSION

Our laser diode current driver design, an improvement upon the Hall–Libbrecht design,[2] has extremely good long-term stability, low noise, fast modulation response, and fast response to load impedance changes. The implementation of a digital set-point circuit and the use of modern surface-mount chips has resulted in more than an order-of-magnitude improvement in noise and stability. It also allows for extremely precise repeatability, high accuracy, and the ability to control the current set point remotely without degrading the performance of the current driver. The device outperforms any commercial device we are aware of, yet is simple and inexpensive enough to be used as a "laboratory standard" for both highly sensitive as well as less sensitive diode laser applications.

ACKNOWLEDGMENTS

This work was supported by a grant from the Research Corporation and by Brigham Young University's Office of Research and Creative Activities.

[1] C. E. Wieman and L. Hollberg, Rev. Sci. Instrum. **62**, 1 (1991).
[2] K. G. Libbrecht and J. L. Hall, Rev. Sci. Instrum. **64**, 2133 (1993).
[3] P. Horowitz and W. Hill, *The Art of Electronics*, 2nd ed. (Cambridge University Press, Cambridge, England, 1997).
[4] AD8671/AD8672/AD8674 Datasheet (http://www.analog.com/UploadedFiles/Data_Sheets/AD8671_8672_8674.pdf).
[5] LT1028 Datasheet (http://www.linear.com/pc/downloadDocument.do?navId=H0,C1,C1154,C1009,C1026,P1234,D3480).
[6] AD5541/AD5542 Datasheet (http://www.analog.com/UploadedFiles/Data_Sheets/AD5541_5542.pdf).
[7] LM117/LM317A/LM317 Datasheet (http://cache.national.com/ds/LM/LM117.pdf).